

Supporting Information

© Wiley-VCH 2014

69451 Weinheim, Germany

**Fine-tuning the Local Symmetry to Attain Record Blocking
Temperature and Magnetic Remanence in a Single-Ion Magnet****

Liviu Ungur, Jennifer J. Le Roy, Ilia Korobkov, Muralee Murugesu, and Liviu F. Chibotaru**

anie_201310451_sm_miscellaneous_information.pdf

Contents

1	Experimental and Synthetic Details	1-2
2	Single Crystal X-ray Crystallography	2-2
3	SQUID Magnetometry	3-4
4	Quantum Chemical Calculations	4-6
4.1	Computational Details	4-6
4.2	Ab initio study of the Er complex	4-8
4.3	Ab initio study of the Dy complex	4-10
4.4	Analysis of the multiplet-specific crystal-field for Er and Dy compounds	4-12
4.5	Calculations on symmetrized models of Er compounds. Influence of distortions..	4-15

1 Experimental and Synthetic Details

Synthesis of [K(18-Crown-6)][Er(COT)₂]. (CCDC reference 961014) C₈H₈ (0.11 mL, 1.0 mmol) was added to K⁰ (82 mg, 2.1 mmol) in 15 mL of 50:50 THF:toluene at -20 °C. The mixture is stirred at -20 °C for 4 hours, filtered, and ErCl₃ (139 mg, 0.51 mmol) was added to the filtrate. The reaction is stirred for 1 hour at -20 °C, an additional 3 h at room temperature, then filtered. 18-crown-6 (132 mg, 0.5 mmol) dissolved in 1 mL of THF was added. Isolated crystals of [K(18-Crown-6)][Er(COT)₂] (306 mg, 74% yield) are extremely air and moisture sensitive. ¹H NMR (400 MHz, CDCl₃) δ (ppm) 5.73 (br.s, 16H, H_{COT}), 1.81 (br.s, 24H, H_{18-crown-6}).

Synthesis of [K(18-Crown-6)][Dy(COT)₂]. (CCDC reference 961013) Complex **2** was prepared in an analogous manor to **1** using C₈H₈ (0.11 mL, 1.0 mmol), K⁰ (82 mg, 2.1 mmol), 18-crown-6 (132 mg, 0.5 mmol), and DyCl₃ (137 mg, 0.51 mmol). Isolated crystals of [K(18-Crown-6)][Dy(COT)₂] (287 mg, 73% yield) are extremely air and moisture sensitive. ¹H NMR (400 MHz, CDCl₃) δ (ppm) 5.73 (br.s, 16H, H_{COT}), 1.81 (br.s, 24H, H_{18-crown-6}).

2 Single Crystal X-ray Crystallography

For **Er** and **Dy** complexes a suitable prism shaped crystal was mounted in inert oil and transferred to the cold gas stream of the diffractometer. Unit cell measurements and intensity data were collected at 200 K on a Bruker-AXS SMART 1 k CCD diffractometer using graphite monochromated MoK_α radiation (λ = 0.71073 Å). The data reduction included a correction for Lorentz and polarization effects, with an applied multi-scan absorption correction (SADABS).¹ The crystal structure was solved and refined using the SHELXTL² program suite. Direct methods yielded all non-hydrogen atoms, which were refined with

¹ G. M. Sheldrick, SADABS — Bruker AXS area detector scaling and absorption, version 2008/1, University of Göttingen, Germany **2008**.

² G. M. Sheldrick, *Acta Cryst.* **2008**, A64, 112.

anisotropic thermal parameters. All hydrogen atom positions were calculated geometrically and were riding on their respective atoms. The crystal structures has been deposited at the Cambridge Crystallographic Data Centre and allocated the deposition numbers CCDC 961013 and 961014.

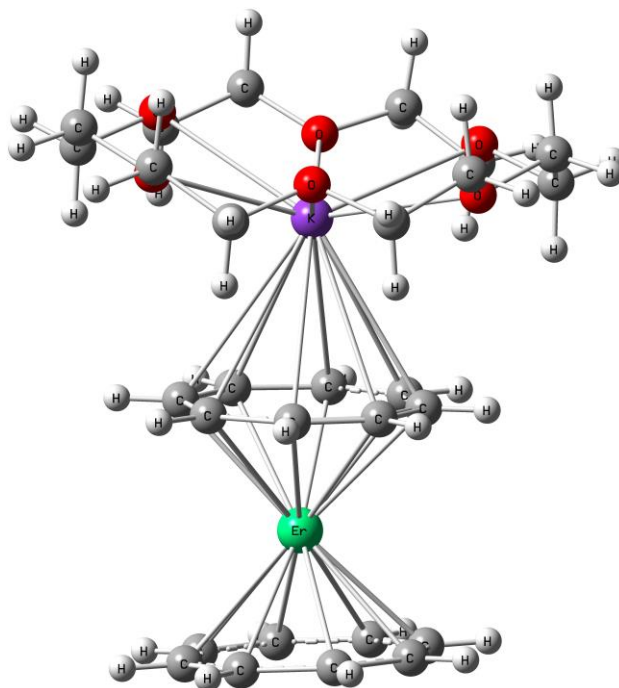


Figure S1. Full molecular structure of the [K(18-Crown-6)][Ln(COT)₂].

3 SQUID Magnetometry

Magnetic susceptibility measurements were obtained using a Quantum Design SQUID magnetometer MPMS-XL7 operating between 1.8 and 300 K for dc applied fields ranging from -7 to 7 T. Ac susceptibility measurements were carried out under an oscillating ac field of 3 Oe and ac frequencies ranging from 1 to 1500 Hz. and at 0 dc field. Hysteresis measurements were performed using hysteresis mode and in all measurements data was collected starting at H=0 Oe, sweeping to H=50 kOe and then cycling to H= -50 kOe and back to H=50 kOe. Reported sweep rates reflect the average sweep rate calculated per cycle. Diamagnetic corrections were applied for the sample holder and the core diamagnetism from the sample (estimated with Pascal constants).

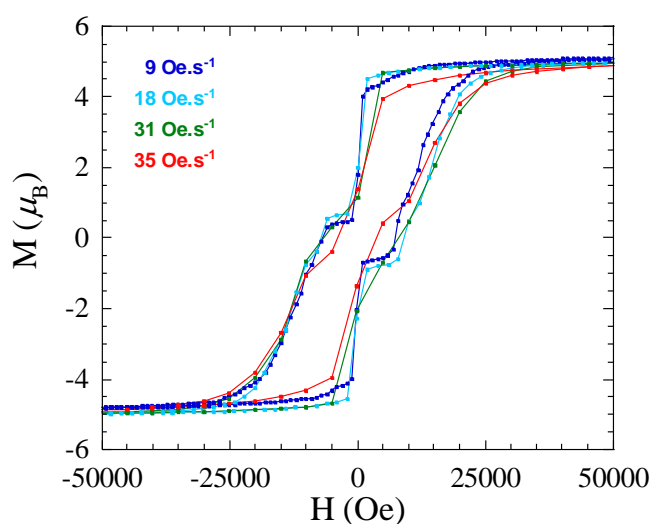


Figure S2. Sweep rate dependence of the magnetization hysteresis at 1.8 K for $[\text{Er}(\text{COT})_2]$.

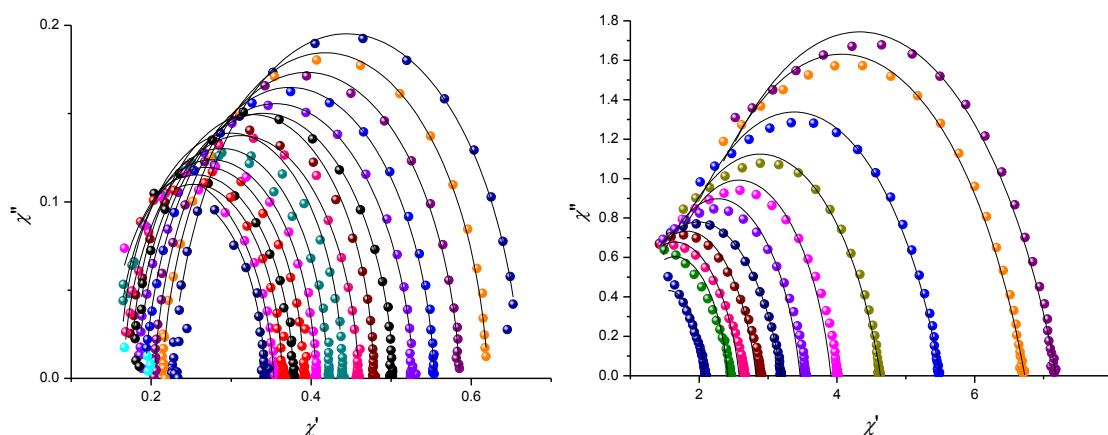


Figure S3. Cole-Cole plot for zero field ac susceptibility of $[\text{Er}(\text{COT})_2]$ (left) and $[\text{Dy}(\text{COT})_2]$ (right). Experimental data points are represented by circles and the solid black line represents a fit to the data. $[\text{Er}(\text{COT})_2]$ α^2 values: 0.08 (15K), 0.07 (16K), 0.07 (17K), 0.06 (18K), 0.07 (19K), 0.05 (20K), 0.009 (21K), 0.05 (22K), 0.002 (23K), 0.007 (24K), 0.03 (25K), 0.008 (26K), 0.03 (27K),

0.004 (28K), 0.07 (29K), 0.02 (30K). $[\text{Dy}(\text{COT})_2]^- \alpha^2$ values: 0.43 (1.8K), 0.42 (2K), 0.39 (2.5K), 0.37 (3K), 0.23 (3.5K), 0.22 (4K), 0.36 (4.5K), 0.24 (5K), 0.24 (5.5K), 0.18 (6K), 0.13 (7K).

4 Quantum Chemical Calculations

4.1 Computational Details

All calculations were done with MOLCAS 7.8 and are of CASSCF/RASSI/SINGLE_ANISO type.

Three structural approximations of the initial LnCOT₂K molecules were employed: **A** (small), **B** (medium) and **C** (the entire molecule).

In the structural model **A**, the K atom and its surroundings were removed.

The structural model **B**, included the structure of the model A and the K atom, while the surrounding of the K atom was removed.

The structural model **C**, is the entire molecule as determined experimentally (taken from the CIF file).

The structure of the models **A** and **B** is shown in Figure S4 and Figure S5, respectively.

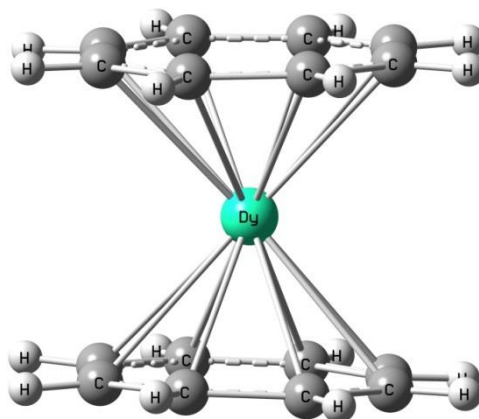


Figure S4. Structure of the model A.

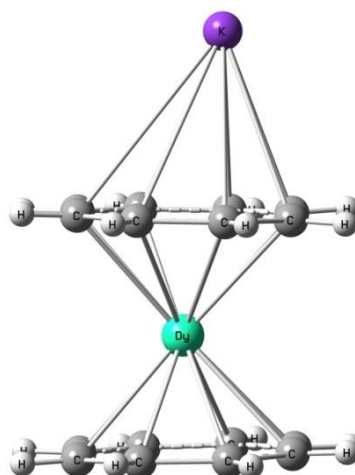


Figure S5. Structure of the model B.

Two basis set approximations have been employed: **1** – small, **2** – large; Table shows the contractions of the employed basis sets for all elements.

All in all there are 6 computational models for each magnetic center in the considered LnCOT₂K molecule: **A1**, **A2**, **B1**, **B2**, **C1** and **C2**.

Alongside the above compounds with real geometry, the symmetrized D_{8d} or D_{8d} versions of the structural model **A1** and **A2** were computed.

Table S1. Contractions of the employed basis sets in computational approximations.

	Basis 1 (DZP-quality)	Basis 2 (TZP-quality)
<u>employed for models A</u>	Ln.ANO-RCC...7s6p4d2f1g. C.ANO-RCC...3s2p1d. H.ANO-RCC...2s1p.	Ln.ANO-RCC...8s7p5d3f2g1h. C.ANO-RCC...4s3p2d1f. H.ANO-RCC...3s2p1d.
<u>employed for models B</u>	Ln.ANO-RCC...7s6p4d2f1g. K.ANO-RCC...5s4p1d. C.ANO-RCC...3s2p1d. H.ANO-RCC...2s1p.	Ln.ANO-RCC...8s7p5d3f2g1h. K.ANO-RCC...6s5p2d1f. C.ANO-RCC...4s3p2d1f. H.ANO-RCC...3s2p1d.
<u>employed for models C</u>	Ln.ANO-RCC...7s6p4d2f1g. K.ANO-RCC...5s4p1d. O.ANO-RCC...3s2p. C.ANO-RCC...3s2p1d.(close) C.ANO-RCC...3s2p.(distant) H.ANO-RCC...2s1p. (close) H.ANO-RCC...2s. (distant)	Ln.ANO-RCC...8s7p5d3f2g1h. K.ANO-RCC...6s5p2d1f. O.ANO-RCC...3s2p. C.ANO-RCC...4s3p2d1f. (close) C.ANO-RCC...3s2p.(distant) H.ANO-RCC...3s2p1d. (close) H.ANO-RCC...2s. (distant)

Ln= Dy, Er

Active space of the CASSCF method includes the electrons from the last shell spanning the 7 orbitals (4f orbitals of the Ln³⁺ ion).

For Er compound all spin states were mixed by the spin-orbit coupling, while for Dy only a limited number of roots was possible to mix, namely 21 sextets, 128 quartet and 130 doublet states.

On the basis of the resulting spin-orbital multiplets the SINGLE_ANISO program computed local magnetic properties (*g*-tensors, main magnetic axes, local magnetic susceptibility, Crystal-Field parameters, etc.)

4.2 Ab initio study of the Er complex

Table S2. Energy of the lowest spin-orbit Kramers doublets (cm^{-1}).

Er						
	A1	A2	B1	B2	C1	C2
	0.0	0.0	0.0	0.0	0.0	0.0
	180.6	171.9	186.7	178.3	183.3	175.3
	244.7	187.7	258.6	201.8	250.8	194.0
	320.2	267.6	330.6	278.2	324.7	272.9
	406.3	389.4	408.7	392.6	407.2	392.5
	435.9	392.0	440.8	396.8	437.8	395.3
	522.8	491.3	523.6	492.3	523.2	494.0
	543.2	515.1	540.9	513.7	541.1	516.0
	6650.5	6600.4	6652.2	6602.3	6651.1	6601.4
	6871.2	6810.9	6873.9	6815.7	6872.2	6814.5
	6910.6	6813.0	6921.0	6822.1	6915.0	6817.1
	6956.5	6861.1	6965.0	6869.8	6960.0	6865.8
	7013.2	6936.6	7016.0	6941.6	7014.2	6940.2
	7028.5	6949.4	7032.9	6952.3	7030.1	6952.2
	7072.5	6994.5	7073.5	6996.3	7072.2	6996.7
	10755.7	10696.6	10758.0	10699.1	10756.6	10698.1
	10935.5	10861.6	10937.9	10870.0	10936.2	10866.2
	10956.6	10869.0	10965.0	10872.3	10960.0	10871.5
	10985.6	10895.6	10992.4	10902.8	10988.3	10899.7
	11010.9	10936.4	11014.4	10940.5	11012.2	10939.8
	11031.2	10951.4	11034.1	10954.8	11031.8	10953.9
	13554.6	13502.1	13557.0	13504.8	13555.5	13503.8
	13649.4	13571.7	13659.9	13582.5	13653.8	13576.9
	13720.0	13665.3	13725.3	13670.9	13722.0	13668.8
	13789.9	13719.1	13793.7	13723.3	13791.2	13722.2
	13877.5	13816.0	13877.1	13816.1	13876.6	13817.8
	18954.6	19027.0	18957.1	19029.3	18955.7	19028.5
	19025.5	19095.1	19028.3	19097.9	19026.6	19097.1
	19150.4	19212.7	19153.6	19216.0	19151.7	19215.3
	19262.7	19286.6	19272.7	19296.5	19267.4	19292.3

Table S3. g tensors of the low-lying Kramers doublets (KD) for the Er compound.

Er							
	A1	A2	B1	B2	C1	C2	
1	g_x	0.00000	0.00000	0.00000	0.00000	0.00000	0.00000
	g_y	0.00000	0.00000	0.00000	0.00000	0.00000	0.00000
	g_z	17.95773	17.95907	17.95777	17.95903	17.95729	17.95873
2	g_x	0.00009	0.00093	0.00013	0.00010	0.00019	0.00026
	g_y	0.00009	0.00112	0.00013	0.00018	0.00019	0.00046
	g_z	15.53831	15.53196	15.53751	15.53448	15.53654	15.52985
3	g_x	9.97860	9.95661	10.01673	9.99209	10.02976	9.98612
	g_y	9.14018	9.15824	9.13694	9.16463	9.11107	9.15281
	g_z	1.21744	1.22260	1.21655	1.21905	1.21776	1.22243
4	g_x	0.29126	0.28133	0.31048	0.29629	0.33916	0.31044
	g_y	0.54306	0.51838	0.56517	0.53064	0.57624	0.52584
	g_z	3.65613	3.65644	3.65303	3.65261	3.65373	3.65580
5	g_x	0.00185	0.01372	0.00185	0.00013	0.00263	0.00277
	g_y	0.00269	0.03880	0.00298	0.00492	0.00342	0.01891
	g_z	13.09594	11.27766	13.09317	12.61454	13.09325	12.06628
6	g_x	0.07122	0.04751	0.07167	0.05911	0.05582	0.04030
	g_y	0.19322	0.13744	0.19579	0.16995	0.19562	0.15305
	g_z	6.10644	7.92912	6.08840	6.56323	6.09101	7.11934
7	g_x	0.01542	0.02935	0.00837	0.02693	0.01297	0.03193
	g_y	0.04115	0.05232	0.03945	0.05348	0.04639	0.06036
	g_z	10.96192	10.03568	11.13371	10.05190	11.07041	10.00648
8	g_x	0.02111	0.01626	0.02302	0.01760	0.02608	0.01970
	g_y	0.04530	0.02540	0.05286	0.02764	0.05603	0.02911

g_z	13.22919	12.82185	13.15779	12.77257	13.15557	12.71848
-------	----------	----------	----------	----------	----------	----------

Table S4. Angles between the main magnetic axes of the lowest Kramers doublet obtained in different computational approximations (degrees).

	A1	A2	B1	B2	C1	C2
A1	0.0000	0.0485	0.1259	0.0048	0.1107	0.0183
A2	0.0485	0.0000	0.1744	0.0533	0.1591	0.0668
B1	0.1259	0.1744	0.0000	0.1211	0.0152	0.1076
B2	0.0048	0.0533	0.1211	0.0000	0.1059	0.0135
C1	0.1107	0.1591	0.0152	0.1059	0.0000	0.0924
C2	0.0183	0.0668	0.1076	0.0135	0.0924	0.0000

Table S5. Angles between the main magnetic axes of the lowest and first excited Kramers doublets obtained in different computational approximations (degrees).

	A1	A2	B1	B2	C1	C2
	0.9111	0.9359	0.9307	1.0129	0.9610	1.0120

4.3 Ab initio study of the Dy complex

Table S6. Energy of the lowest spin-orbit Kramers doublets (cm^{-1}).

Dy						
	A1	A2	B1	B2	C1	C2
	0.0	0.0	0.0	0.0	0.0	0.0
	19.0	21.1	13.7	23.5	17.0	22.3
	47.9	46.4	40.0	41.7	45.4	45.4
	50.6	91.4	52.9	82.9	52.0	89.3
	64.6	121.7	54.5	112.3	59.7	118.5
	86.1	144.5	74.8	134.4	81.8	142.3
	266.3	219.3	275.5	227.1	270.9	223.0
	975.3	913.8	976.3	912.8	975.9	916.2
	3557.3	3563.2	3552.8	3559.4	3555.3	3562.0
	3575.1	3584.0	3567.5	3580.1	3571.8	3582.7
	3598.8	3598.4	3595.4	3592.5	3597.8	3597.2
	3615.1	3639.1	3604.6	3629.3	3610.8	3636.5
	3693.6	3664.3	3693.4	3663.6	3694.0	3664.8
	3849.8	3796.6	3852.4	3798.0	3851.5	3798.0
	4255.3	4172.7	4258.8	4174.5	4257.1	4175.6
	6072.6	6074.5	6065.1	6067.9	6069.3	6072.3
	6089.7	6090.1	6082.8	6083.9	6087.0	6088.6
	6126.2	6115.8	6122.4	6112.6	6124.7	6115.3
	6247.1	6220.9	6244.4	6218.4	6246.1	6220.8
	6403.7	6353.9	6402.5	6351.9	6403.5	6354.2
	6626.2	6535.4	6630.5	6538.0	6628.4	6538.2
	8035.9	8023.8	8029.0	8017.9	8033.0	8021.9
	8056.1	8040.6	8051.3	8036.4	8054.3	8039.8
	8127.7	8101.0	8125.7	8099.4	8127.0	8101.1
	8319.4	8275.5	8316.0	8271.6	8318.2	8275.0
	8530.5	8434.9	8534.3	8437.2	8532.4	8437.5
	9570.2	9544.7	9565.3	9542.8	9568.1	9544.2
	9582.9	9562.4	9578.9	9556.8	9581.4	9561.0
	9754.5	9712.7	9752.0	9709.8	9753.6	9712.3
	9912.6	9930.7	9909.3	9927.1	9911.3	9929.9

Table S7. *g* tensors of the low-lying Kramers doublets (KD) for the Dy compound.

Dy							
	A1	A2	B1	B2	C1	C2	
1	<i>g_x</i>	0.15885	0.06799	0.22048	0.09193	0.15078	0.06229
	<i>g_y</i>	0.33286	0.14494	0.47607	0.17816	0.34203	0.14464
	<i>g_z</i>	12.52391	12.74732	12.04372	12.01527	12.54628	12.64381
2	<i>g_x</i>	0.51429	0.00055	0.72538	0.02950	0.52275	0.00019
	<i>g_y</i>	0.90395	0.05016	1.31624	0.11451	0.92303	0.05849
	<i>g_z</i>	9.48267	14.03975	9.20168	13.57053	9.39675	13.84353
3	<i>g_x</i>	2.86129	0.09691	4.98428	0.14316	5.84099	0.08350
	<i>g_y</i>	5.09444	0.27690	4.99390	0.30686	4.59491	0.25147
	<i>g_z</i>	7.42136	9.78195	5.59399	10.27602	3.27272	9.98272
4	<i>g_x</i>	0.05027	3.58611	0.26689	3.74556	0.85046	3.13895
	<i>g_y</i>	0.95748	3.66266	4.69720	3.95213	1.33352	3.17226
	<i>g_z</i>	9.64508	6.11609	11.05393	6.08306	13.77715	6.18857
5	<i>g_x</i>	1.84535	2.57420	1.64811	2.55063	1.91068	2.61576
	<i>g_y</i>	4.74326	4.44672	5.21917	4.21625	5.51024	4.95524
	<i>g_z</i>	15.37925	13.18670	11.90127	13.37072	14.52371	12.80990
6	<i>g_x</i>	0.05721	0.35862	0.15696	0.36985	0.06068	0.33842
	<i>g_y</i>	0.09192	1.15866	0.18810	1.20250	0.09756	1.07666
	<i>g_z</i>	19.42521	18.46002	19.42635	18.47093	19.40685	18.50342
7	<i>g_x</i>	0.00005	0.00020	0.00007	0.00012	0.00000	0.00001
	<i>g_y</i>	0.00010	0.00028	0.00010	0.00034	0.00005	0.00057
	<i>g_z</i>	17.44995	17.44501	17.44807	17.44400	17.44865	17.44368
8	<i>g_x</i>	0.00000	0.00000	0.00000	0.00000	0.00000	0.00000
	<i>g_y</i>	0.00000	0.00000	0.00000	0.00000	0.00000	0.00000

g_z	19.88854	19.89009	19.88988	19.89159	19.88859	19.89013
-------	----------	----------	----------	----------	----------	----------

Table S8. Angles between the main magnetic axes of the lowest Kramers doublet obtained in different computational approximations (degrees).

	A1	A2	B1	B2	C1	C2
A1	0.0000	0.1634	6.9953	11.9258	0.9103	1.0822
A2	0.1634	0.0000	6.8476	11.7788	1.0500	0.9349
B1	6.9953	6.8476	0.0000	4.9317	7.8961	5.9134
B2	11.9258	11.7788	4.9317	0.0000	12.8276	10.8443
C1	0.9103	1.0500	7.8961	12.8276	0.0000	1.9848
C2	1.0822	0.9349	5.9134	10.8443	1.9848	0.0000

Table S9. Angles between the main magnetic axes of the lowest and first excited Kramers doublets obtained in different computational approximations (degrees).

	A1	A2	B1	B2	C1	C2
	14.8273	24.0766	11.2771	7.7741	16.0850	21.3744

4.4 Analysis of the multiplet-specific crystal-field for Er and Dy compounds

Recently, the extraction of the parameters of the multiplet-specific crystal-field for lanthanides methodology has been implemented in the SINGLE_ANISO program in MOLCAS. The results presented below use the ab initio CASSCF/RASSI wave function and energies to compute the parameters of the crystal-field splitting of the ground J multiplet.

The Crystal-Field Hamiltonian:

$$H_{CF} = \sum_{k,q} B_k^q O_k^q$$

where:

O_k^q -- Extended Stevens Operators (ESO) as defined in:

1. Rudowicz, C.; J. Phys. C: Solid State Phys., 18 (1985) 1415-1430.

2. Implemented in the "EasySpin" function in MATLAB, www.easyspin.org.

k - the rank of the ITO, = 2, 4, 6.

q - the component (projection) of the ITO, = $-k, -k + 1, \dots, 0, 1, \dots, k$;

Quantization axis was chosen the main magnetic axis of the ground Kramers doublet.

Table S10. Parameters of the Crystal-Field acting on the ground atomic multiplet $J=15/2$ for the Er compound.

k	q	experimental geometry (model C2)	symmetrized model A2 point group D_{8d}
2	-2	-0.14590823E-03	--
	-1	-0.45326802E+00	--
	0	-0.15179209E+01	-0.16128301E+01
	1	0.13084287E-04	--
	2	0.10790289E+00	--
4	-4	-0.76372172E-06	--
	-3	0.57676159E-03	--
	-2	-0.84070180E-05	--
	-1	0.63497076E-02	--
	0	-0.12333653E-01	-0.14164906E-01
	1	-0.66223309E-04	--
	2	0.83199485E-03	--
	3	0.29522453E-05	--
4	-0.43484894E-03	--	
6	-6	0.27575836E-07	--
	-5	0.96081660E-04	--
	-4	-0.96922005E-08	--
	-3	0.24234307E-04	--
	-2	-0.17019085E-06	--
	-1	-0.66047718E-04	--
	0	0.62788540E-04	0.84827470E-04
	1	0.88629361E-06	--
	2	-0.72309807E-05	--
	3	0.91503101E-08	--
	4	-0.11452407E-04	--
	5	-0.37788586E-07	--
6	-0.17655975E-05	--	

Table S11. Parameters of the Crystal-Field acting on the ground atomic multiplet J=15/2 for the Dy compound.

k	q	experimental geometry (model C2)	symmetrized model A2 point group D _{8d}
2	-2	-0.48489380E-01	--
	-1	-0.27590446E+00	--
	0	0.35092959E+01	0.34858335E+01
	1	0.27793871E-01	--
	2	-0.29984534E+00	--
4	-4	0.74867351E-03	--
	-3	-0.36015637E-03	--
	-2	-0.14385499E-03	--
	-1	0.17989150E-02	--
	0	0.18623546E-01	0.17514148E-01
	1	-0.53556948E-04	--
	2	-0.89884093E-03	--
	3	0.80032542E-04	--
4	0.22448714E-02	--	
6	-6	-0.36527336E-05	--
	-5	-0.51906111E-04	--
	-4	-0.68670933E-05	--
	-3	0.14839339E-05	--
	-2	-0.59268265E-06	--
	-1	0.46400246E-05	--
	0	0.50937669E-04	0.48555395E-04
	1	0.50822469E-07	--
	2	-0.38473610E-05	--
	3	-0.38434243E-06	--
	4	-0.20592483E-04	--
	5	0.22002072E-04	--
6	-0.69400391E-05	--	

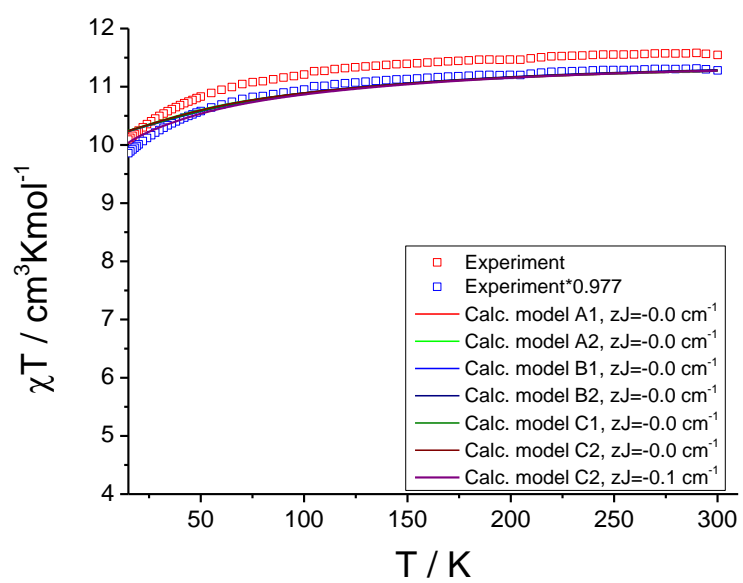


Figure S6. A comparison of the measured and calculated molar magnetic susceptibility of the Er compound. zJ parameter accounts for the mean field effect of the crystal environment.

4.5 Calculations on symmetrized models of Er compounds. Influence of distortions.

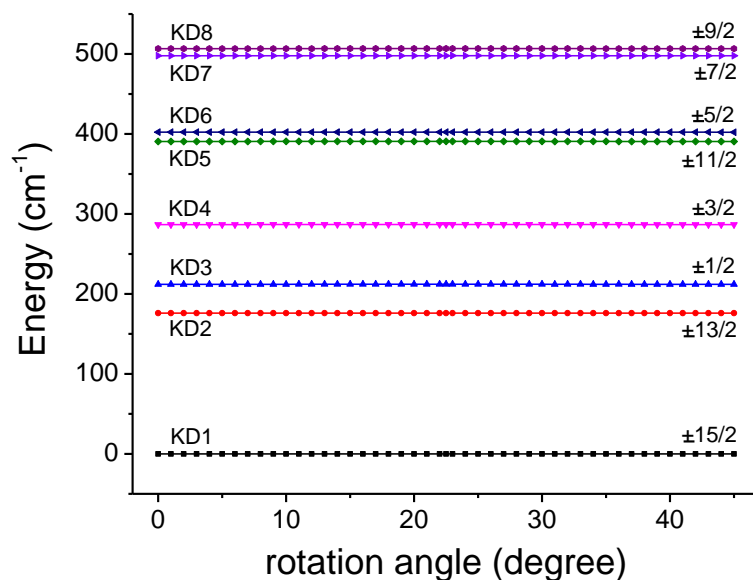


Figure S7. Energy levels as function of the rotation angle of one COT ring around the symmetry axis of the compound. All points correspond to ab initio calculations of CASSCF/RASSI type similar to the model A2 described above.

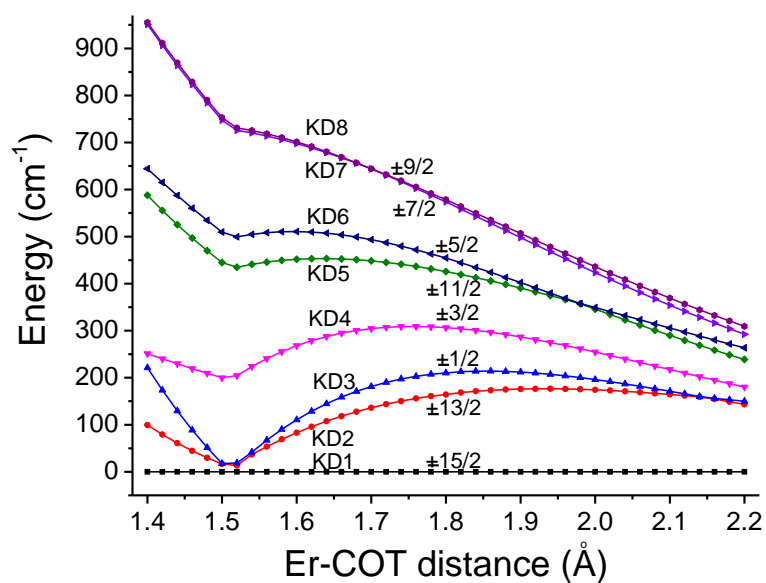


Figure S8. Energy levels as function of the Er-COT distance (assumed equal for both COT rings). All points correspond to ab initio calculations of CASSCF/RASSI type similar to the model A2 described above.